Ecological Engineering 78 (2015) 41–52

Contents lists available at ScienceDirect

Ecological Engineering

journal homepage: www.elsevier.com/locate/ecoleng

Quantifying nutrient and suspended solids fluxes in a constructed tidal marsh following rainfall: The value of capturing the rapid changes in flow and concentrations

J. Randall Etheridge, François Birgand*, Michael R. Burchell II

North Carolina State University, Biological and Agricultural Engineering, Campus Box 7625, Raleigh, NC 27695, USA

ARTICLE INFO

Article history:
Received 1 November 2013
Received in revised form 28 April 2014
Accepted 5 May 2014
Available online 15 June 2014

Keywords:
Constructed tidal marsh
Nutrient retention
Tides
Rainfall event
UV–vis spectrometer

ABSTRACT

Coastal tidal wetlands are perceived to provide nutrient dissipation services and serve as the final buffer between excess nutrient loads coming from nearby upland watersheds and sensitive estuarine waters. The construction and restoration of tidal marshes has the potential to benefit coastal waters. However, the water quality services of tidal wetlands have yet to be established with any certainty. This is in part due to the difficulty of monitoring these systems where flow and concentrations vary widely with tidal ebb and flood along with rainfall events mobilizing nutrients in pulses from upstream watersheds. In this article, we show over a period of 10 days following a rainfall event, the value of high temporal resolution data to characterize the complex nutrient and flow dynamics and to reliably calculate material balances in a created coastal marsh in North Carolina. Ultraviolet–visible spectrometers were used to obtain 15-min concentration data for nitrate, total Kjeldahl nitrogen, dissolved organic carbon, total suspended solids, phosphate, and total phosphorus. Our results show that a pulse of nitrate moved through the marsh from upstream agricultural production following the rainfall event and 25% (13 kg of 53 kg) of the nitrate was retained in the marsh over a period of 10 days. No other material showed a clear pulse from the upstream agricultural production. The marsh acted as a sink for total suspended solids (40 kg) and had near neutral mass balances for dissolved organic carbon, total Kjeldahl nitrogen, total phosphorus, and phosphate. Subsequent simulations indicated that different and erroneous results would have been obtained from 2-, 6- or 12-h sampling intervals. These results demonstrate, even on a short term basis, why high-frequency data acquisition is necessary in these tidal marsh systems to truly quantify their impact on water quality ecosystem services.

1. Introduction

Quantifying and understanding the role that tidal marshes play in coastal energy and nutrient dynamics has been a focus of research since the introduction of the marsh outwelling theory (Teal, 1962; Odum, 1968). Gaining a clearer understanding of the ecosystem services provided by coastal marshes, both natural and constructed, has increased in importance due to continued marsh loss from sea level rise and coastal development. Many different approaches have been taken to quantify the ecosystem services of nutrient and suspended solids retention including monitoring the fluxes at the inlet/outlet of marshes (e.g. Dame et al., 1991; Jordan and Correll, 1991; Gardner and Kjerfve, 2006) and modeling the biogeochemical processes (Aziz and Nedwell, 1986; Anderson et al., 1997). The highly dynamic nature of systems with tidal flow makes it difficult to capture the variations in nutrient concentrations and process rates over multiple tidal cycles.

Improvements in technology and new methods give present day researchers many advantages over previous attempts to quantify the nutrient and suspended solids fluxes in tidal systems. Equipment that can be installed on-site for automated monitoring makes possible the collection of water quality parameters at a frequency unimaginable in the past due to the cost of sample collection and analysis. Monitoring of water quality at a high temporal resolution in upland watersheds has been used to gain information on residence times and diurnal variations in chemical concentrations (Kirchner et al., 2000; Pellerin et al., 2012). Recently developed portable ultraviolet–visible (UV–vis) spectrometers have made possible the collection of water quality parameters including, but

* Corresponding author. Tel.: +1 919 513 2499; fax: +1 919 515 7760.
E-mail addresses: jretheri@gmail.com (J.R. Etheridge), francois_birgand@ncsu.edu (F. Birgand), mike_burchell@ncsu.edu (M.R. Burchell II).

http://dx.doi.org/10.1016/j.ecoleng.2014.05.021
0925-8574/

not limited to, nitrate (NO_3—N), total Kjeldahl nitrogen (TKN), dissolved organic carbon (DOC), phosphate (PO_4—P), total phosphorus (TP), and total suspended solids (TSS) at a high temporal resolution in brackish tidal waters (Etheridge et al., 2014).

A common theme throughout the literature examining sediment fluxes in coastal marshes is the influence of storm conditions on sediment delivery to marshes (Jordan et al., 1986; Cahoon, 2006; Turner et al., 2006). Many of these published accounts referred to extreme tropical weather systems with storm surges and increased wave action, but the importance of rainfall events in shaping marshes and driving biogeochemical processes should not be overlooked (Day et al., 2002). For instance, Whiting et al. (1989) noted an increase in the export of all forms of nitrogen when their sample collection occurred following rainfall events. The increase in NO_3—N and ammonium (NH_4—N) concentrations was attributed to high concentrations of these solutes in the rain. Particulate nitrogen, mobilized when rain impacted the marsh surface, showed the largest increase in concentration following storm events. Pulses of DOC and particulate organic carbon were observed by Chalmers et al. (1985) following rainfall events, and the particulate fraction showed the greatest increase in concentrations. These studies show the importance of capturing storm events when trying to understand coastal marsh nutrient dynamics in marshes that have few inputs from upstream sources.

The flux of nutrients derived from within coastal wetlands is small compared to the nutrient input from urban or agricultural sources when these sources are present. Whiting et al. (1989) noted an increase in NO_3—N concentrations of less than 0.4 mg L^{-1} due to rainfall, whereas Poe et al. (2003) found that NO_3—N concentrations in a coastal wetland receiving agricultural drainage increased by a minimum of 2.8 mg L^{-1} during each monitored rainfall event. A portion of the nutrients applied to agricultural fields as fertilizer are mobilized by both surface and subsurface flow, discharging to surface waters that flow toward coastal wetlands. Agricultural drainage systems, which are required to maximize yields on poorly drained coastal soils, increase the rate at which nutrients leave these facilities. The combination of elevated nutrient concentrations and increased flows following rainfall events can cause substantial fluxes of these nutrients to downstream aquatic systems (including coastal wetlands) in short periods of time (e.g. Birgand et al., 2011). Therefore, a high proportion of the annual nutrient delivery to wetlands may result from just a few rainfall events (Raisin et al., 1997; Jordan et al., 2003).

The goal of this work was to examine water quality data collected at a high temporal resolution in a created brackish marsh in the 10 days following an April 2012 rainfall event, to demonstrate how nutrient and suspended solids dynamics could be described in detail. The nutrient and suspended solids retention or release was quantified using a mass balance approach to determine whether the marsh was a source or sink for nutrients and suspended solids during the short term event. Simulations of 2-h, 6-h, and 12-h sampling intervals were run to additionally demonstrate the potential error induced by less frequent sample collection and the value of near continuous concentration data.

2. Methods

2.1. Site description

The study site was a constructed marsh in Carteret County, North Carolina (34.82°N 76.61°W). The marsh and tidal stream system was located between a row crop agricultural production facility to the north and the upper reaches of the North River to the south. The agricultural operation grew crops such as corn, soybeans, and wheat and was drained using 1 m deep parallel ditches placed 80 m apart. The area was a natural wetland until it was drained and converted to agricultural production in the late 1970's as North River Farms. During the fall of 2005 and the spring of 2006, 6.9 ha of brackish marsh and 1000 m of tidal stream were constructed on a portion of the land (Fig. 1). The goal of the marsh construction was to create habitat equivalent to that available in natural marshes, while improving the quality of water reaching the North River estuary. The stream and marsh were designed using reference-based design principles. To achieve target elevations, significant grading was required. Topsoil was stockpiled during excavation and replaced during final grading to provide suitable conditions for plant establishment. The constructed marsh was planted with *Spartina alterniflora*, *Spartina patens*, and *Juncus roemerianus* at appropriate elevation ranges based on observations from local reference marshes.

Drainage from the agricultural land was directed into the constructed marsh with the idea that biogeochemical processes occurring in the constructed system would remove a portion of the nutrients before the water reached the sensitive estuarine ecosystem. A portion of the agricultural drainage flowing in a large canal just west of the site was diverted into one of the constructed streams, Broome's Branch, by a low level rock weir. This constructed tidal stream discharged to the estuary, but was linked to the same drainage canal at the southern end of the project, creating a hydraulic loop. Drainage from the agricultural production also entered the constructed system through Evans' Creek which transitioned from a freshwater stream at its northernmost point to a brackish stream a few hundred meters northeast of its confluence with Broome's Branch.

The constructed system was monitored to quantify the nutrient retention capacity of the created marsh/tidal stream system and gain insight into the nutrient dynamics in the marsh. The focus of this research was on 5.6 ha of tidal marsh adjacent to 660 m of Broome's Branch (Fig. 1). An upstream/downstream monitoring design was used to calculate a mass balance for the portion of the constructed system located between the two monitoring stations. This reach of tidal stream was chosen as there were no major inputs of surface water to the marsh other than through the two monitoring stations. Measurements of flow and nutrient concentrations at the upstream station (closest to the drainage canal diversion) and the downstream station (closest to the estuary) were required to calculate the mass balance for the marsh.

2.2. Flow and rainfall monitoring

Measuring flow (Q) in tidal systems creates challenges not faced in upland systems with unidirectional flow. Bi-directional flow due to tides prevents the use of stage-discharge curves. The flow through each monitoring station was calculated using the continuity equation ($Q = VA$) from 15-min data.

Five-meter long trapezoidal flumes fitted with ramps were installed at each monitoring station to funnel bidirectional flow over a section of known and constant geometry to lower uncertainties in velocity (V) and wetted cross sectional area (A) measurements. These flumes should not be confused with the flumes used in conducting studies on the marsh platform (e.g. Wolaver et al., 1983; Whiting et al., 1989). The cross section (A) was calculated from water levels measured above the flume bottom using pressure transducers (ISCO 750 and ISCO 6712, Lincoln, NE, USA; Infinities USA, Port Orange, FL, USA) and digital imagery (GaugeCam, Raleigh, NC, USA). The flume bottom elevation at the upstream station was 0.02 m (NAD83) and the flume bottom elevation at the downstream station was −0.49 m (NAD83).

Measured bidirectional velocities at the center of the flume (ISCO 750 and ISCO 6712, Lincoln, NE, USA) were taken as index

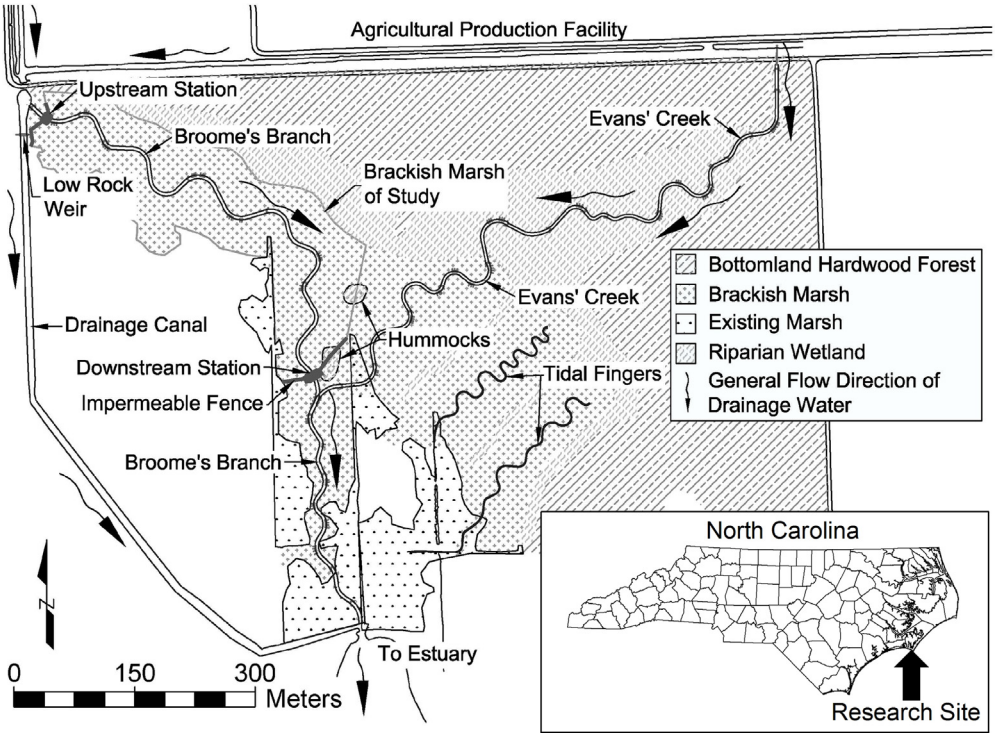

Fig. 1. Design schematic of the brackish marsh and surrounding restored wetland ecosystems, constructed on an area that was previously in agricultural production. Other than the area denoted as existing marsh, the whole shaded area was previously in agricultural production. The study reach was located between the two monitoring stations (noted as Brackish Marsh of Study).

velocities (Levesque and Oberg, 2012; ISO 15769(E), 2012) and correlated to the section-averaged mean velocities (V) obtained from manual gauging using the velocity area method (ISO 748, 1997). Manual velocity measurements were made using a portable velocity meter (Marsh-McBirney, Frederick, MD, USA).

To avoid flow bypassing the flumes at high tide, an impermeable fence (1 mm thick reinforced polypropylene) was installed from the flumes to the upper elevations of the marsh. The impermeable fence was anchored a minimum of 15 cm below the soil surface and directed all the water on the marsh surface to flow through the flumes. Visual inspection of the fence during site visits showed it was effective for preventing flow from bypassing the monitoring stations.

Rainfall was measured both automatically every 15 min (Model 07852, Davis Instruments, Hayward, CA, USA fitted with an event data logger HOBO, Bourne, MA, USA) and manually on a biweekly basis. Automatic cumulative rainfall amounts were adjusted to those of the manual measurements.

2.3. Water quality monitoring

The equipment and calibrations used to monitor the water quality in the constructed system along with the challenges faced in using the new technology have previously been described (Etheridge et al., 2013, 2014). Briefly, in-situ portable UV–vis spectrometers (spectro::lyser, s::can Measuring Systems, Vienna, Austria) were installed at each monitoring station in March 2011. The initial installation of the spectrometers in the stream resulted in substantial chemical fouling that prevented quality data from being collected. To address this problem, the spectrometers were removed from the stream and stream water was pumped to the instruments. The combination of reduced exposure to the stream water and the addition of a pressurized freshwater cleaning reduced the fouling and allowed quality data to be collected between service intervals. The rainfall event in this study was the first major rainfall (42 mm) following the installation of the final working configuration of the anti-fouling system. Each station was also equipped with a multi-parameter sonde (Manta2 model, Eureka Environmental Engineering, Austin, TX) in line with the spectrometer to measure salinity and dissolved organic matter fluorescence (FDOM; Cyclops-7 model, Turner Designs, Sunnyvale, CA, USA).

Etheridge et al. (2014) demonstrated development of site specific calibrations of the spectrometer and sonde using laboratory analyzed discrete samples to obtain 15-min data on NO_3—N, TKN, DOC, PO_4—P, TP, and TSS concentrations. Ammonium (NH_4—N) concentrations could not be derived with this method as they were always found to be below the detection limit (0.1 mg L^{-1}). Calibrations were developed using the discrete samples and partial least squares regression (PLSR) for each of the parameters (Table 1) using the pls package (Mevik et al., 2011) in the R software (R Core Team, 2013). When the NO_3—N and PO_4—P concentration output from the PLSR model were below the detection limit of the instrument (0.1 mg L^{-1} and 0.01 mg L^{-1}, respectively), the concentrations were automatically set at one-half of the detection limit.

2.4. Mass balance

A mass balance approach (i.e. the difference between the inflow and outflow) was used to determine whether the constructed tidal marsh was a sink or a source of TSS and nutrients. The mass balances for each material at each monitoring station was calculated using the following equation:

$$M = k\sum_{i=1}^{i=t} q_i c_i \Delta t \quad (1)$$

Table 1
Details of the models used to estimate water quality parameters from the measured absorption spectra. This table was adapted from and details can be found in Etheridge et al. (2014).

Parameter	Sensor data used in calibration	R^2	Root mean square error of prediction (mg L^{-1})	Number of components
NO_3—N	1st Derivative of raw spectrum	0.998	0.1	14
TKN	1st Derivative of raw spectrum and FDOM	0.91	0.27	10
TKN	1st Derivative of turbidity compensated spectrum*	0.86	0.33	11
DOC	Turbidity compensated spectrum and FDOM	0.94	1.3	13
DOC	1st Derivative of turbidity compensated spectrum*	0.93	1.3	12
TSS	Raw spectrum	0.92	7.3	6
PO_4—P	Turbidity compensated spectrum	0.66	0.01	18
TP	1st Derivative of raw spectrum	0.73	0.024	14
Salinity	1st Derivative of raw spectrum	0.97	1.8	12

* Used only if FDOM measurements were not available.

where M is the total mass either exported or imported at the monitoring station (g), t is time (min), k is a constant for converting units, q_i and c_i are the 15-min water flow rates ($m^3\ s^{-1}$) and concentrations (mg L^{-1}) at time i, respectively. For the purpose of calculating the mass balance, at each station all inputs to the marsh were considered positive (+) and exports from the marsh negative (−).

The impact of nitrogen wet deposition during the event was checked due to the influence shown by Whiting et al. (1989). The event mean concentrations of NO_3—N and NH_4—N were available for the week of April 3, 2012 through April 10, 2012 at a National Atmospheric Deposition Program (2013) monitoring site (NC06) located less than 8 km from the research site. The mass of inorganic nitrogen deposited on the marsh during the event was calculated by multiplying the event mean concentrations, the rainfall depth, and the marsh area.

2.5. Simulating sampling at lower frequencies

A major strength of this study was the availability of nutrient concentrations at 15-min intervals. To evaluate the value of sampling at high frequencies, longer sampling intervals were simulated and the resulting mass balances calculated over the 10-day period for NO_3—N and DOC. In previous marsh studies, reported sampling frequencies regularly ranged between 0.5-h and 2-h, and conclusions were reached after monitoring very few tidal cycles (Chrzanowski et al., 1982; Wolaver et al., 1988; Whiting et al., 1989; Gardner and Kjerfve, 2006; Tzortziou et al., 2008). Sampling as infrequent as daily has been suggested as potentially useful for calculating fluxes of suspended solids when paired with water level monitoring and a hypsometric model of the marsh (Gardner et al., 1989). Sampling intervals of 2-h, 6-h, and 12-h were simulated using the R software (R Core Team, 2013) to coincide with the range used in previous studies and the frequencies of 1–2 samples per tidal cycle. The starting time for each simulation was randomly chosen to begin within the first sampling window of each frequency, for example the 2-h simulations could start at any point during the first two hours of the monitoring period. The times of all the other simulated sample collections occurred at regular intervals after the random starting time. For a true continuous chemograph and for a given sampling frequency, one could theoretically create an infinite number of chemographs based on an infinite number of starting points. The data used in this study was collected every 15-min and only provided eight potential starting points for a 2-h sampling frequency. To increase the number of potential starting points within the first sampling window, the original data was transformed into 1-min data by linear interpolation. From the 1-min data (which contain the same information as the 15-min data), 120 simulations were carried out for each sampling frequency for NO_3—N and DOC. One hundred twenty simulations were used as this was the maximum number of starting points available for the 2-h sampling interval using the 1-min data. To calculate loads from the simulated sampling results, synthetic chemographs were generated by linear interpolation between simulated consecutive samples, which associated a concentration value with each flow value using Eq. (1). The 15-min flow data was used in this simulation as the collection of flow data at this frequency or a higher frequency is often carried out with lower frequency water sampling.

3. Results and discussion

From April 5, 2012 at 5 PM until April 6, 2012 at 3:45 PM, 42 mm of rain fell at the research site. This study focuses on the period of time from April 6, 2012 at 5:15 AM until April 16, 2012 at 2:00 AM, which included 19 complete tidal cycles. The start and end times were chosen when the water level reached a minimum and the tide was changing from ebbing to flooding. Using the same point on the tidal cycle at the lowest water levels minimizes errors in mass balance calculations that could be caused by having different volumes of water remaining in the marsh. The starting time was prior to the arrival of the nitrate pulse and the ending time followed the NO_3—N concentrations returning to below the detection limit. The peak flow rate and peak NO_3—N concentration both occurred during the study period.

3.1. Flow

The stage-velocity and stage-flow relationships at the downstream station were examined for the tidal cycle that began at 9:30 PM on April 11, 2012 as this cycle represents what occurred under normal flow conditions (Fig. 2a). The flow rate asymmetry and surge in flow during the flooding and ebbing tides has been observed in previous studies of coastal marshes (e.g. Boon, 1975; Bayliss-Smith et al., 1979). The surges have generally occurred in other marshes at the point where water begins to spread over the marsh platform (bankfull stage) on the flooding tide and on the ebbing tide when the water level in the stream goes below bankfull stage (Fagherazzi et al., 2013). During this cycle, the peak flows occurred when the stage was above 0.75 m, which is 0.25 m above bankfull stage.

Normal tidal functioning was dramatically affected by the arrival of drainage water following the 42 mm storm event. Tidal asymmetry is still clearly visible, but peak velocities, stages, flow rates and overall volume exchanged were much greater during the tide which began at 6:15 PM on April 6, 2012 (Fig. 2b). The same 0.75 m stage threshold applied following storm events where flow and velocities changed dramatically above and below this stage. The volume of water exchanged during this tidal cycle was more

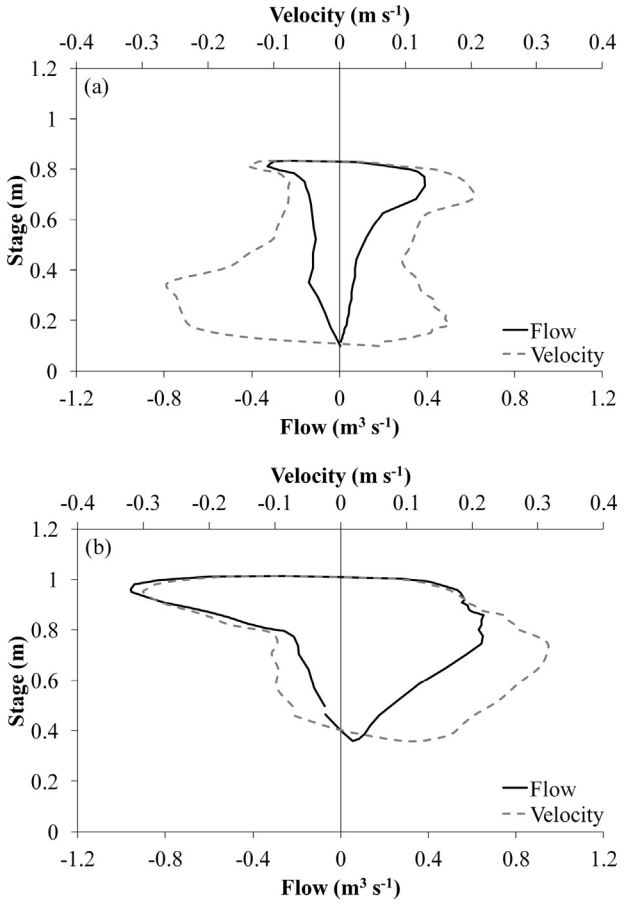

Fig. 2. Stage-velocity and stage-flow rate relationships at the downstream station for tidal cycles during a) normal, non-storm event (flooding tide began at 9:30 PM on April 11, 2012) and b) following a rainfall event (flooding tide began at 6:15 PM on April 6, 2012). Note: Positive (+) flow rate and velocity was toward the estuary. Negative (−) flow rate and velocity was into the marsh.

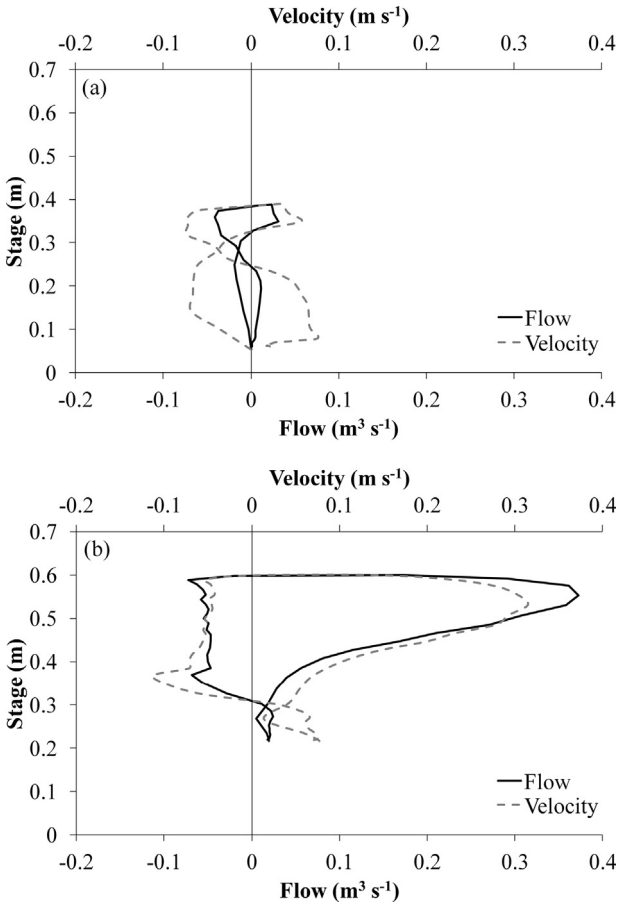

Fig. 3. Stage-velocity and stage-discharge relationships at the upstream station (a) tidal cycle where the flooding tide began at 12:00 AM on April 12, 2012 (b) tidal cycle where the flooding tide began at 6:30 PM on April 6, 2012. Positive (+) flow rate and velocity was into the marsh. Negative (−) flow rate and velocity was toward the agricultural drainage canal.

than 3 times greater (19,700 m^3 vs. 6,100 m^3) than the tide during normal flow conditions.

The upstream station was located at the northern node of the hydraulic loop formed by Broome's Branch and the drainage canal west of the marsh. Two flow scenarios were observed at the upstream station during this study. Under normal tidal flow on the flooding tide, the time for estuarine water to reach the node through the canal was shorter than through the marsh, and created a scenario where this water entered the marsh through the upstream station (positive flow into the marsh). Once the water level and flow in the marsh were high enough, flow was reversed and water discharged north through the upstream station back into the canal. This phenomenon, specific to the hydraulic loop, created "figure-8-shaped" stage-flow relationships (Fig. 3a). During periods where agricultural drainage was impacting the marsh following rainfall, more water came from the upstream agricultural drainage system, but the tides would still reverse the flow of this increased volume and created the highest positive flows (from the drainage canal into the marsh) at the upstream station during the flooding tide (Fig. 3b). In fact, for 5.5 h on the flooding tide following the April 5–6th rainfall event, the marsh was simultaneously being filled from upstream and downstream (Figs. 2b and 3b). These dynamic flow scenarios demonstrated the importance of documenting and measuring instantaneous flow to close the water balance in the marsh. The same reasoning applied to material loads.

3.2. Nutrient and TSS dynamics

3.2.1. Dynamics at the upstream station

The flow dynamics which mixed water from the estuary, the marsh, and the upstream watershed produced similarly complex nutrient dynamics. Prior to the rainfall, NO_3—N concentrations in the tidal stream were below the detection limit of 0.1 mg L^{-1}. The general pattern of concentration over the 10-day period was that the NO_3—N concentration peaked quickly following rainfall and then slowly returned to concentrations below the detection limit of the spectrometer over 10 days (Fig. 4a). The influx of NO_3—N to the marsh is believed to result from the typical leaching of the drained agricultural soils in late spring (Birgand, 2000; Birgand et al., 2011). Poe et al. (2003) found similar pulsing of NO_3—N in their monitoring of a nearby constructed wetland designed with the sole purpose of treating nutrients from agricultural runoff and drainage. The NO_3—N concentrations measured in the marsh following the rainfall event were substantially higher than the NO_3—N concentrations measured in other marsh studies, including those that monitored following rainfall, showing the influence anthropogenic sources of nutrients can have on coastal ecosystems (e.g. Whiting et al., 1989; Gardner et al., 2006).

Nutrient dynamics at the tidal scale revealed complex mixes of water of different origins, as evidenced by a series of concentration peaks and troughs not necessarily in phase with the hydraulic observations noted earlier. Arrival of the storm drainage water was

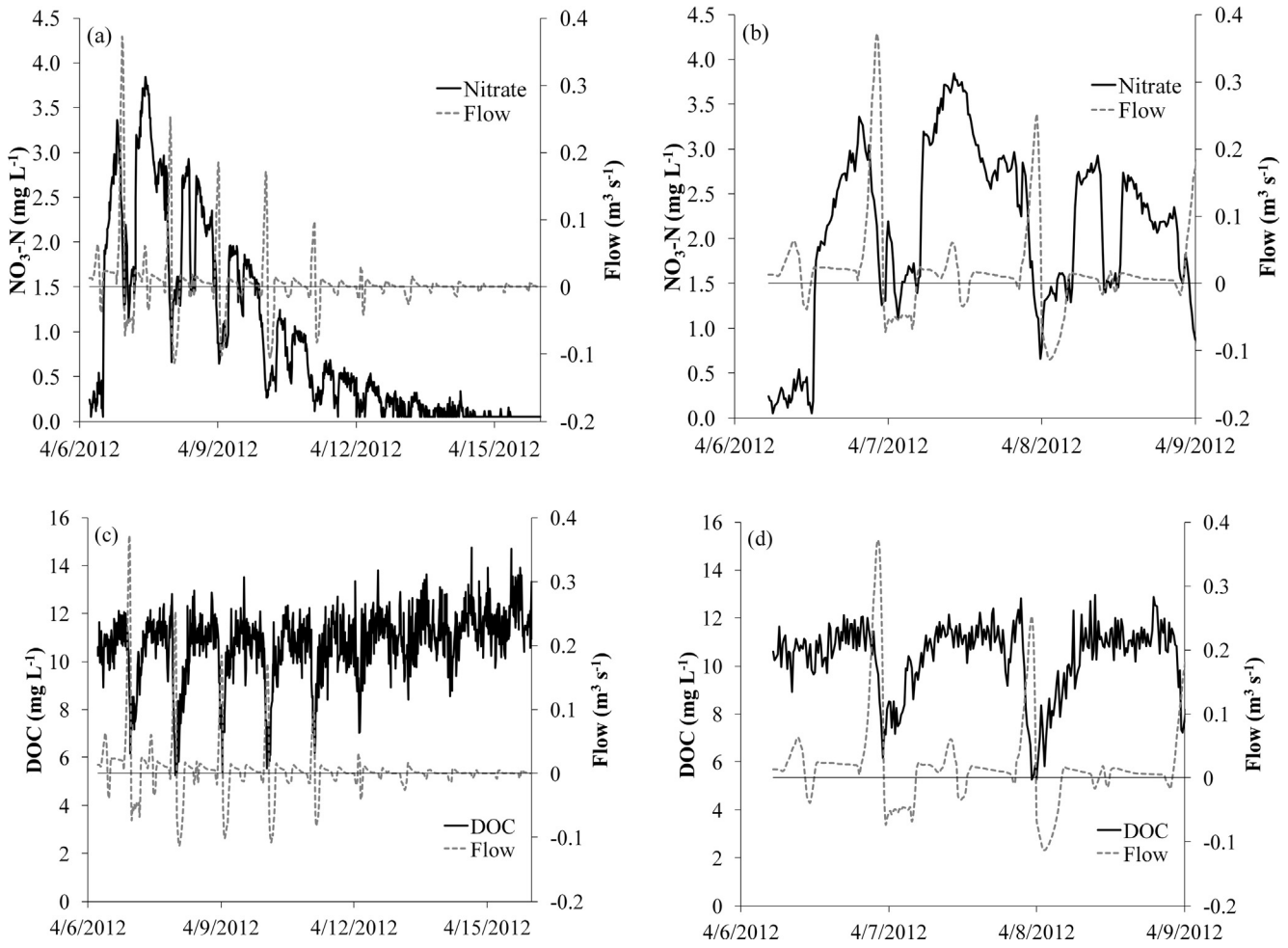

Fig. 4. Monitoring results at the upstream station (a) NO_3—N concentrations and flow for the whole monitoring period (b) NO_3—N concentrations and flow for the first 3 days of the monitoring period (c) DOC concentrations and flow for the whole monitoring period (d) DOC concentrations and flow for the first 3 days of the monitoring period. Note: Positive (+) flow rates indicate flow into the marsh and negative (−) flow rates indicate flow toward the agricultural drainage canal.

associated with the sudden increase in concentrations from less than 0.5 mg L^{-1} to 2 mg L^{-1} when the flow became positive (i.e. into the marsh) during the middle of the day on April 6, 2012 (Fig. 4b). However, water entering the marsh at the upstream station quickly became a mixture of drainage and estuarine waters as evidenced by the sudden nitrate concentration decreases and troughs (accompanied by salinity increases, data not shown) during the following highest flow peaks. As the flow became negative, a smaller spike in NO_3—N concentrations showed a different mixture of estuarine water and the agricultural drainage water pushed out of the marsh through the upstream station and back into the canal.

The DOC concentrations did not exhibit the pulsed nature shown by NO_3—N indicating that the upstream watershed was not a large additional source of DOC to the marsh during this event (Fig. 4c). Dissolved organic carbon concentrations rose toward the end of the monitoring period as the influence of estuarine and upland sources of water were reduced and the autochthonous DOC became more apparent. The increase in DOC concentrations show that this young marsh was a DOC rich environment compared to the estuary. The most noticeable characteristic of the DOC dynamics at the tidal scale was the decreased concentration when there was a large spike in flow coming from the drainage canal into the upstream station, which was attributed to estuarine water pushing up the canal (Fig. 4d). When the flow reversed and became negative, the DOC concentrations slowly increased as the estuarine water that had been exposed to the DOC rich marsh flowed out of the upstream station.

3.2.2. Dynamics at the downstream station

Similar to the upstream station, the observed series of concentration peaks and troughs were evidence of complex mixtures of waters of different origins at the downstream station. Concentration peaks in phase with ebbing flow were attributed to the NO_3—N enriched drainage waters making their way to the downstream station through the marsh (Fig. 5a). On the following flooding tides (Fig. 5b), concentration peaks were attributed to different nitrate sources either coming from Evans' Creek (as confirmed by a dye tracer study), itself connected to NO_3—N laden waters, or corresponding to a slug of water from the drainage canal which would have had time to go around the created hydraulic loop. The sudden decreases in NO_3—N concentration were attributed to estuarine water on the subsequent flooding tides.

The DOC concentrations were the highest at the downstream station on the first ebbing tide (Fig. 5c). This could have been caused by rainfall feeding additional surface and subsurface flow in the marsh (Chalmers et al., 1985) as it does not coincide with the arrival of drainage waters. The lowest DOC concentrations occurred when the estuarine water was flowing into the marsh on the following flooding tide (Fig. 5d). The increased concentrations occurred on the outgoing tide when water from the upstream watershed or the

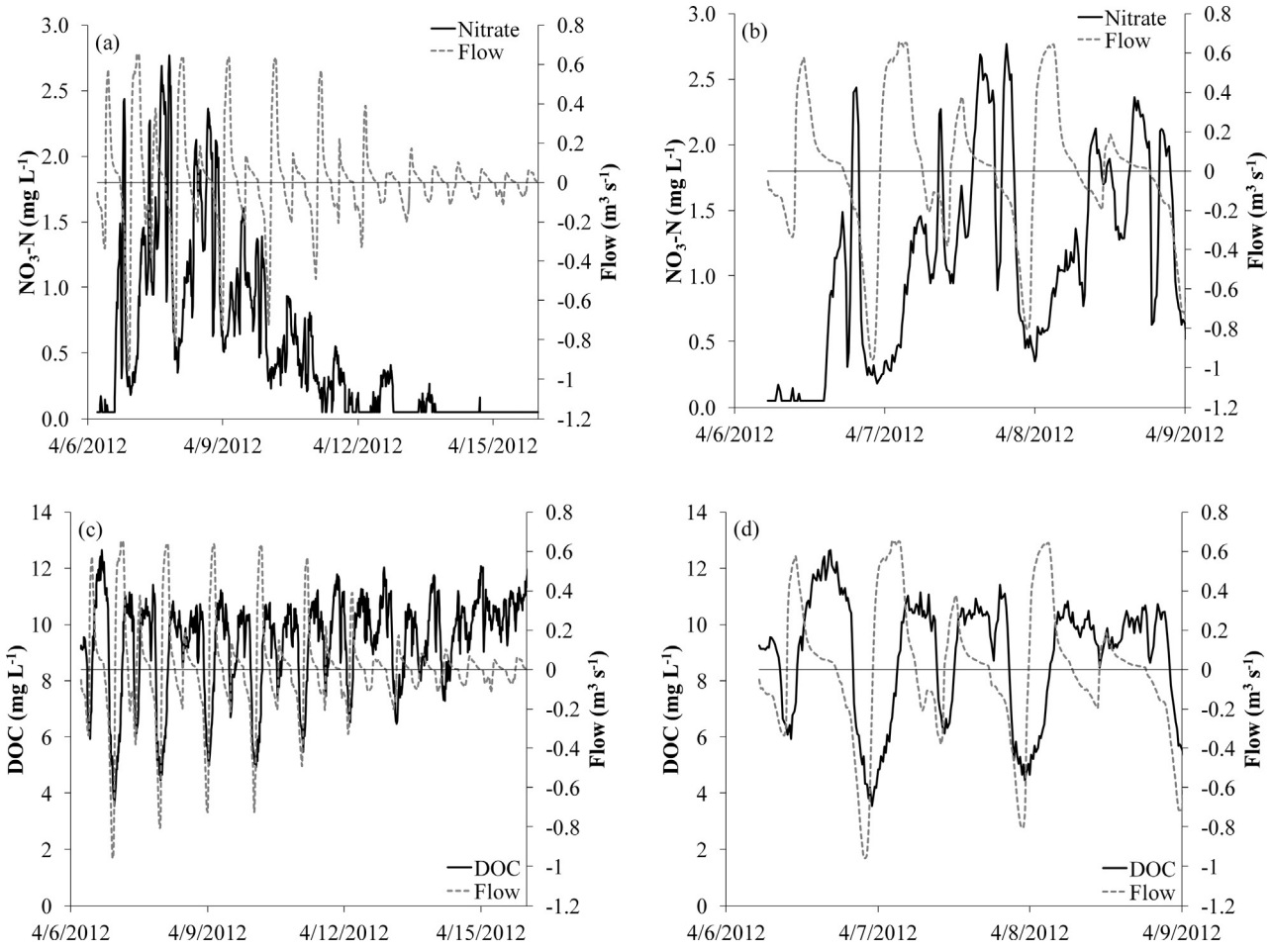

Fig. 5. Monitoring results at the downstream station (a) NO_3—N concentrations and flow for the whole monitoring period (b) NO_3—N concentrations and flow for the first 3 days of the monitoring period (c) DOC concentrations and flow for the whole monitoring period (d) DOC concentrations and flow for the first 3 days of the monitoring period. Note: Positive (+) flow rates indicate flow toward the estuary and negative (−) flow rates indicate flow toward the marsh.

marsh was flowing out of the downstream station. The TKN dynamics at the downstream station (data not shown) were similar to the DOC dynamics, which indicated that TKN was likely in dissolved form rather than in particulate form during the monitoring period.

The range of TP concentrations was the lowest during the first 5 days of the monitoring period when the influence of the storm flow was the greatest (Fig. 6a). The concentrations seemed to be diluted by the large increase in water volume from the agricultural drainage. The highest concentrations occurred near the end of the monitoring period at the end of the ebbing tide when flow rates were low (Fig. 6b). The TP concentrations increased on the first tidal cycle following rainfall similar to the DOC concentrations. The PO_4—P concentration dynamics at the downstream station (data not shown) were nearly opposite of the TP dynamics. Phosphate concentrations increased with the increased influence of estuarine water and decreased as water flowed from the marsh or the upstream watershed. These results indicated that the upstream agricultural production was not a large source of phosphorus to downstream waters.

Similar to TP, an apparent dilution of TSS concentrations was observed during the drainage water pulse through the marsh (Fig. 6c) confirming the mostly subsurface origin of water from the upstream agricultural area that was managed with no-till farming practices and water control structures. This differs from previous reports where particulates are generally mobilized by rainfall (e.g. Chalmers et al., 1985; Whiting et al., 1989). After the drainage pulse through the marsh, TSS concentrations exhibited a double peak at low tide, the first one at the end of ebb and the second at the beginning of flood (Fig. 6d), and occurred during increased velocities at these times (Fig. 2a). The TSS and TP concentration increases appear to be in phase suggesting a strong correlation between TP and particulate phosphorus.

3.3. Cumulative loadings and mass balance

For the purpose of calculating the mass balances, instantaneous load accounting was such that any input to the marsh, whether through the downstream or upstream station, was considered positive (import). Any mass leaving the marsh was considered negative (export). Therefore, a cumulative positive mass balance indicated that the marsh was a sink for the material, while a cumulative negative mass balance indicated that the marsh was a source of the material.

All downstream and combined curves for cumulative flow volumes and loadings somewhat resemble hydrographs during the 10-day monitoring period (Fig. 7). The curves' rises and falls represent water and material entering and leaving the marsh, respectively. Cyclic larger and smaller rises/falls in the curves correspond to the higher-high tides and lower-high tides, respectively.

The water balance showed an overall export of water during the first 6 days attributed to excess rainfall stored and slowly released during this period. The flooding tides of days 7 and 10, created

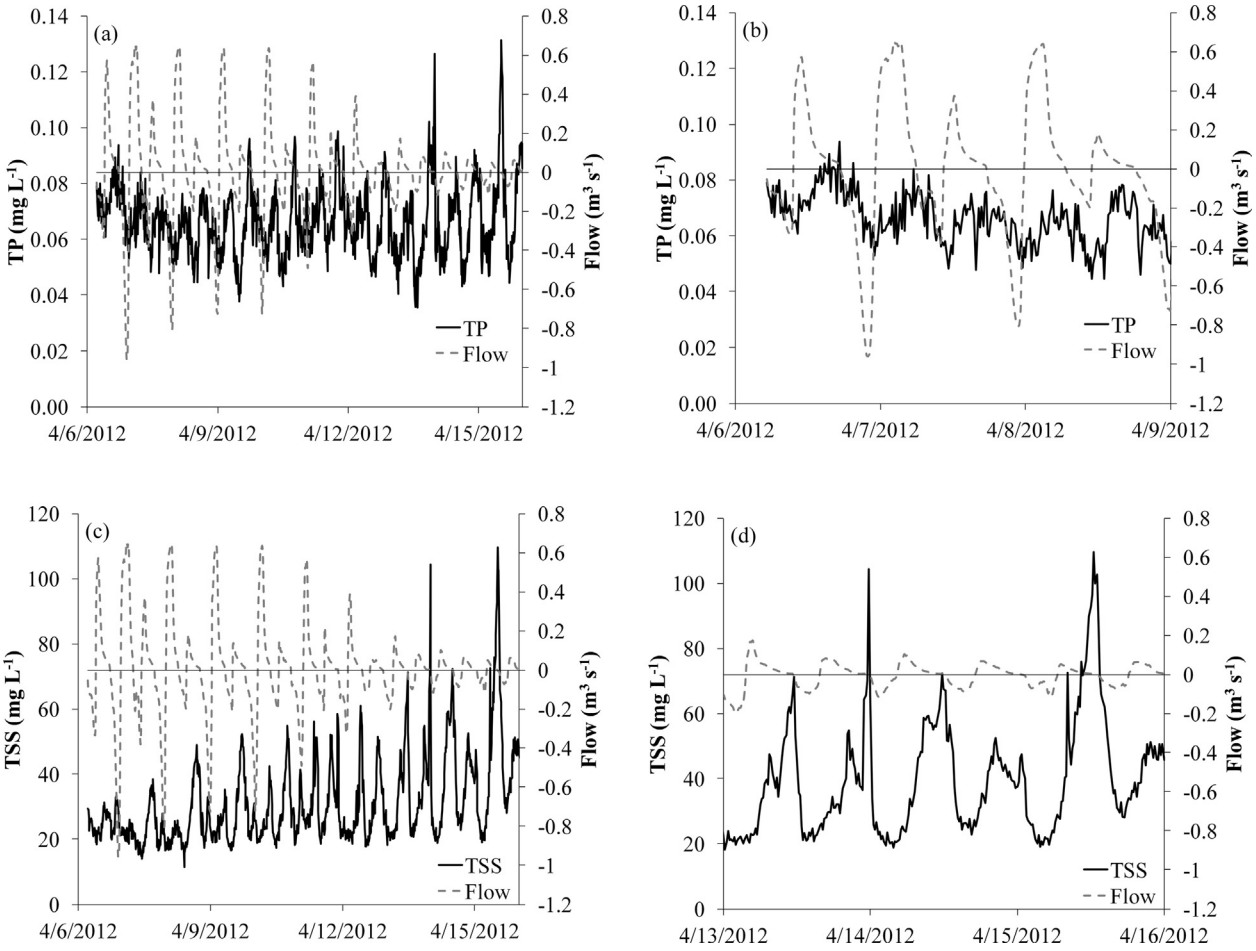

Fig. 6. Monitoring results at the downstream station (a) TP concentrations and flow for the whole monitoring period (b) TP concentrations and flow for the final 3 days of the monitoring period (c) TSS concentrations and flow for the whole monitoring period (d) TSS concentrations and flow for the final 3 days of the monitoring period. Note: Positive (+) flow rates indicate flow toward the estuary and negative (−) flow rates indicate flow toward the marsh.

net water imports in the marsh such that at the end of the study period, there was an import of water corresponding to less than 5% of the total water input to the marsh (Fig. 7a). Measured net water imports during days 7 and 10 could not be attributed to obvious measurement errors and are thought to be real.

The water and nitrate balances followed very different patterns. There was an overall retention or import of 13 kg of nitrate over the 10-day period (Fig. 7b). The nitrate, applied to the agricultural soils and entrained by drainage, entered the marsh from both ends and the net balances were imports of 10 kg at the upstream station and 3 kg at the downstream station. Wet deposition accounted for less than 0.5 kg of inorganic nitrogen input to the marsh surface during the monitoring period. This corresponded to less than 1% of the total input (53 kg) during this event, but should not be ignored, especially in marshes which do not have large anthropogenic inputs of nitrogen (Hopkinson and Giblin, 2008). At the beginning of the monitoring period there was a net negative combined loading for NO_3—N at the downstream station implying that the marsh did not retain all of the NO_3—N that came in through the upstream station in the first few days following the storm event. By day 6, the combined mass balance for the two stations showed retention of 13 kg, which was 25% of the total mass of NO_3—N that entered the marsh (Table 2). We hypothesize that some retention of NO_3—N was due to the processes of denitrification and plant uptake. Plant uptake is generally thought to be the dominant pathway of NO_3—N retention in young constructed marshes and the importance of denitrification increases with marsh maturation (Craft et al., 2003). However, one-third of the overall retention had occurred by the end of the ebbing tide on day 1, which suggests that nitrate was likely physically trapped before it was biogeochemically processed. During this monitoring period at least, the marsh provided the ecosystem service of NO_3—N removal for which it was specifically constructed.

The pattern of import and export for DOC, TKN, TP and PO_4—P more closely followed those of water. The drainage water pulse through the marsh was associated with an overall DOC export until day 5, which was compensated with net imports during the following 5 days (likely driven by the water balance) such that at the end of the 10 day period, there was no significant gain or loss of DOC (Fig. 7c). Export of DOC is expected from marshes on a long term basis (Childers et al., 2002; Tzortziou et al., 2008), and was found to also be the case after several months of monitoring at this site (Etheridge, 2013). The TKN mass balance (data not shown) followed similar trends as the DOC mass balance. The overall balance was a net export of 1 kg of TKN (2% of input) from the system. The export of TKN could have been influenced by the NH_4—N included in the measured TKN concentration. The likely source of TKN was dissolved organic matter leaching from the marsh organic soil and sediment. It is possible that some of the NO_3—N in the marsh was converted to NH_4—N through dissimilatory nitrate reduction to ammonium (DNRA) and then exported from the marsh (Tobias et al., 2001; Koop-Jakobsen and Giblin, 2010), although there were no evidence of corresponding large ammonium exports. The

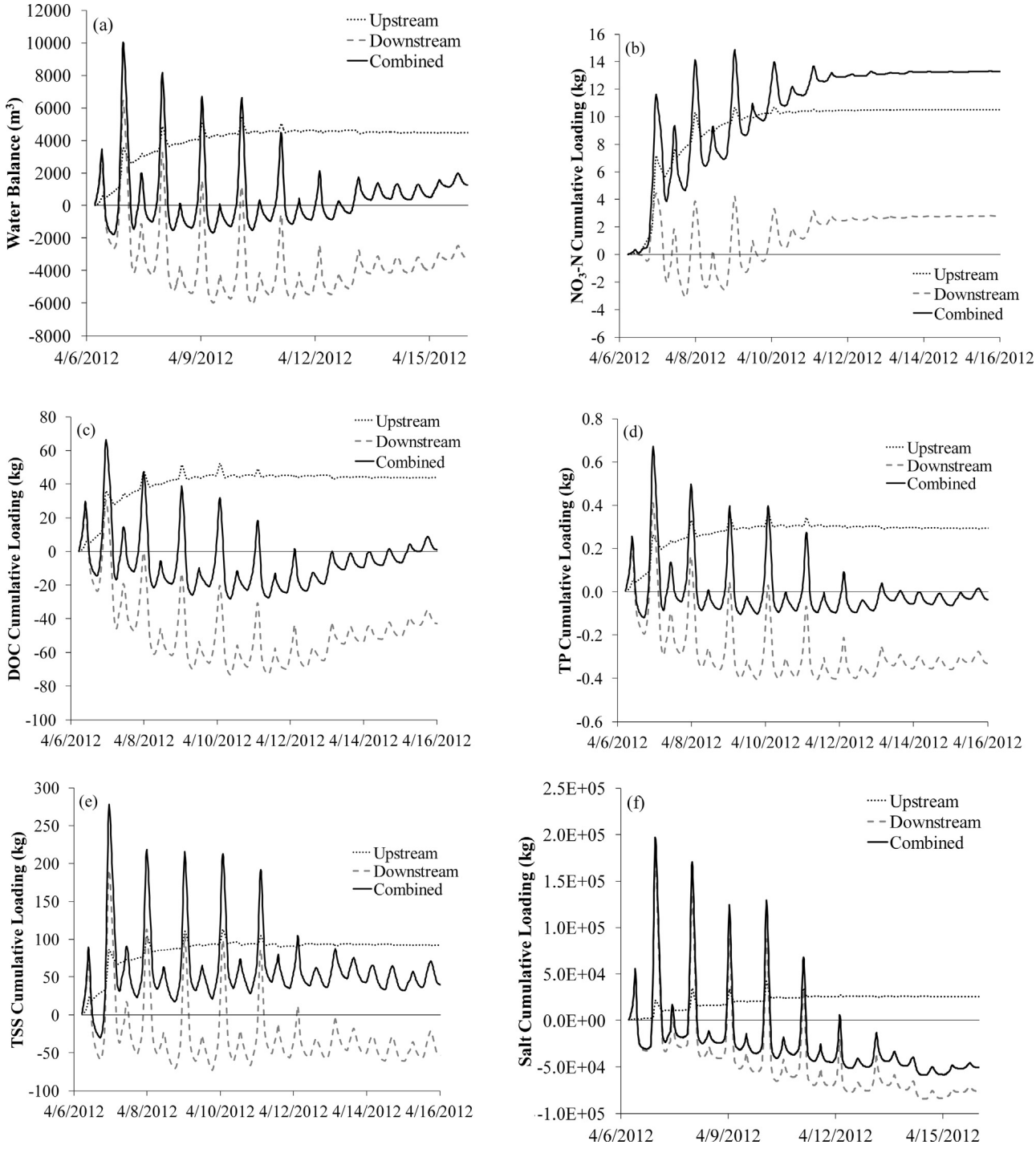

Fig. 7. Upstream, downstream, and combined cumulative balances in the constructed marsh following a rainfall event in April 2012 for (a) water (b) NO_3—N, (c) DOC, (d) TP, (e) TSS, and (f) salt. Positive values indicate retention. Negative values indicate release from the marsh.

Table 2
Mass balance summary for the 10-day monitoring period. A positive mass balance indicates retention and a negative mass balance indicates release by the marsh.

Parameter	Mean concentration (mg L^{-1})		Input mass (kg)	Output mass (kg)	Mass balance (kg)	Percent retention (%)
	Upstream	Downstream				
NO_3—N	0.91	0.52	53	40	13	25
TKN	1.0	0.90	49	50	−1	−2
DOC	10.8	9.4	562	561	1	0
PO_4—P	0.01	0.03	2.11	2.13	−0.02	−1
TP	0.07	0.07	4.4	4.4	0	0
TSS	21	31	1700	1660	40	2

overall mass balances for TP and PO_4—P were nearly neutral despite large fluxes during the tidal cycles (Fig. 7d; Table 2). The similarity in mass balance trends between PO_4—P and TP may seem surprising since their concentration dynamics were opposite, but the fluxes of these nutrients were primarily driven by the water fluxes.

The import and export patterns for TSS differed from those of water. There was a net import of 93 kg (2% of input) during the monitoring period (Fig. 7e). Much of the import occurred during the second tidal cycle on day 1, where most of the TSS load (two-thirds) came from the downstream station. During this cycle, water spent more time on the marsh platform than during any other subsequent tidal cycle. During the drainage pulse, there was a pattern of import at the end of the flooding/ebbing flow of the high-high tide and a pattern of export at the end of the flooding/ebbing flow of the low-high tide. The imports could be due to deposition of TSS as water flooded the marsh platform during the high-high tides. The exports cannot be attributed to water stored in the tidal creek as the water balance was generally neutral at these times. It was expected that TSS would be retained in the marsh due to sedimentation on the marsh surface (Christiansen et al., 2000; Temmerman et al., 2003) as the physical processes impacting sediment deposition begin quickly following vegetation establishment in constructed marshes (Craft et al., 2003). The data suggest that there was a TSS releasing mechanism during low tide fluctuations which must be explored.

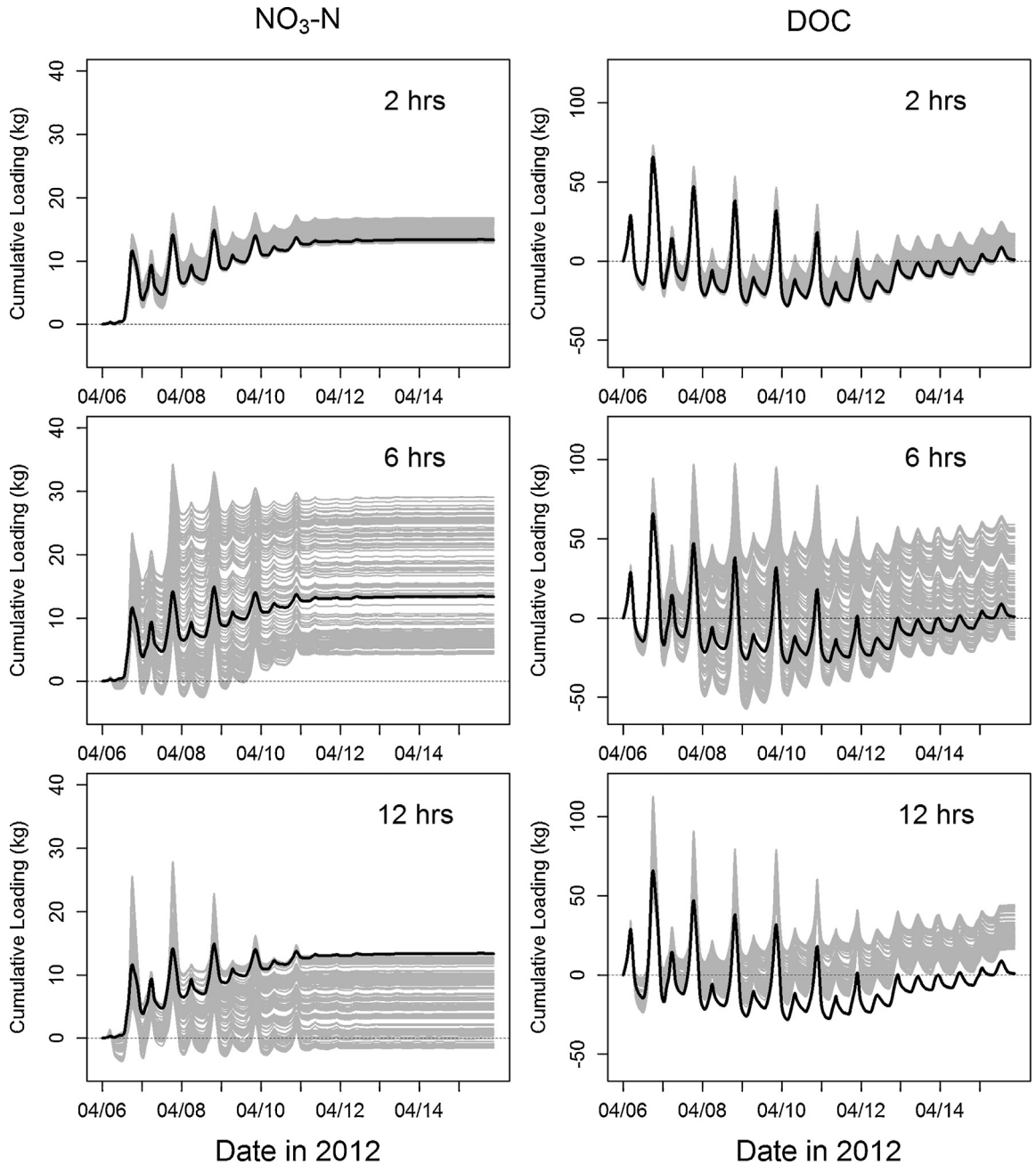

Fig. 8. Comparison of nitrate and DOC balances (left and right columns, respectively) over 10 days between measured (black lines) and 120 simulated (light gray) 2-h, 6-h and 12-h sampling intervals. Each of the 120 simulations is represented by a single gray line, but there is overlapping.

Table 3
Minimum and maximum mass balance results from the sampling frequency simulations. A positive mass balance indicates retention and a negative mass balance indicates release by the marsh.

Sampling frequency	NO_3—N mass balance (kg)		DOC mass balance (kg)	
	Minimum	Maximum	Minimum	Maximum
15-min	13*		0.9*	
2-h	13	17	−0.8	17
6-h	4.3	29	−13	59
12-h	−1.5	13	16	44

* Reference value from monitoring data.

The overall salt balance (Fig. 7f) showed a pattern of export (5% of total fluxes) throughout the study period although much of the overall export occurred during the first large ebb flow associated with the drainage pulse. This pattern of export is opposite to that of water suggesting a possible source of salt for the marsh (Etheridge, 2013). Results from both the water and salt balance suggest that the material movements were not heavily biased by errors in the flow monitoring during the study period. This study included only one event and the magnitude of the fluxes may change in addition to the direction of the fluxes following other storm events, therefore the mass balance results should not be extrapolated to longer periods of time.

The marsh in this study may be a unique case due to the way the marsh was designed and constructed, but these results show the importance of capturing the concentrations of materials entering the marsh from adjacent watersheds. This has been a source of uncertainty in other studies (Jordan and Correll, 1991). The results also show that significant input of NO_3—N can occur from the downstream end of tidal streams. This is most likely to occur in natural marshes if the mouth of a stream or river rich in nutrients discharges to an estuary in close proximity to the mouth of the tidal creek, increasing the potential of mixing.

3.4. Implications for sampling frequency

The primary problem faced in previous attempts to measure nutrient fluxes to characterize ecosystem services in tidal marshes has been uncertainty due to low sampling frequency (e.g. Jordan and Correll, 1991; Gardner and Kjerfve, 2006). Results from this study were used to evaluate the potential errors associated with previous work that collected samples at intervals greater than 15-min or monitored only a few tidal cycles and extrapolated those results to the yearly time scale to estimate marsh nutrient budgets. The cumulative loading results presented here (Fig. 7) clearly show that there is no such thing as a single representative tidal cycle of the 10 day period, since the cycles often yielded very different cumulative loadings. The results also show that the rainfall event drove the short-term (tidal) and midterm (weekly) nutrient balances, especially for NO_3—N.

To further explore the impact of sampling frequency on the mass balance calculations, 2-h, 6-h and 12-h sampling were simulated and the resulting nutrient balance calculated over the 10-day period for NO_3—N and DOC (Fig. 8). For all sampling frequencies, the errors propagated widely after 10 days (Table 3) yielding unreliable results. The differences in the final simulated mass balances from the 15-min sampling data ranged from less than 5% to well over 1000%. The highest percent differences were for DOC as the final mass balance was close to zero. The maximum errors for NO_3—N were above 100%. In some cases the simulated data predicted export while the 15-min reference data showed import. The infrequent sampling regimes created synthetic chemographs that did not capture the concentration peaks and troughs. The 2-h sampling interval showed a systematic overestimation of retention for both NO_3—N and DOC, while the 12-h sampling under- and overestimated retention for NO_3—N and DOC, respectively. There were no systematic trends for the 6-h simulations. Because the 6-h sampling was close to one-half a tidal cycle, the errors were magnified compared to the 12-h sampling. The chemographs produced by a 6-h sampling interval could follow a "sawtooth" or straight line pattern depending on when in the tidal cycle the first sample was taken (data not shown). If the sampling was started at low or high tide a "sawtooth" pattern would be captured as the sampling would show the highest nutrient concentrations near low tide and the lowest nutrient concentrations near high tide. This type of chemograph erroneously assumed a high nutrient concentration during a period when the concentrations were much lower or vice-versa, which resulted in the larger errors for the 6-h sampling interval. The chemographs from the 12-h sampling were more likely to follow a straight line as the sampling frequency nearly matched the tidal frequency and the concentrations were captured at nearly the same point of the tidal cycle throughout the monitoring period. This would likely result in all of the concentrations used in the mass balance calculations to be biased in one direction depending on the nutrient concentration dynamics and result in a lower range of calculated mass balance values than the 6-h sampling frequency.

The actual over- or underestimation trends were probably contingent upon the dataset. The message of this exercise, however, is that in these extremely reactive bidirectional flow systems, data must be acquired often enough to represent actual hydrographs and chemographs. It is possible that 5-min data would have yielded different results than the presented 15-min data. The theoretical error induced by the 15-min data is probably minor compared to those of the less frequent sampling simulated here based on a visual inspection of the hydrographs and chemographs (e.g. in Fig. 5), where the concentration peaks and troughs appear to have been captured.

4. Conclusions

Quantifying the ecosystem service of water quality regulation in created marshes is important to determine how quickly the services develop and the expected water quality impacts of these projects. This study demonstrated methods to quantify nutrient and TSS fluxes over 10 days following a single rainfall event. For this event, the 5-year old constructed marsh in North Carolina retained NO_3—N and had a nearly neutral mass balance for all other parameters measured. Because of infrequent sampling used in previous marsh studies comparison between this study and previous results is difficult. The difference in the final calculated mass balance over 10 days can be over 100% by using a 2-h sampling frequency instead of 15-min sampling frequency. Our method has shown the value of high temporal resolution data without which the complex nutrient and flow dynamics would not have been captured. Our method has also shown the value of high temporal resolution data for obtaining meaningful conclusions on the ecosystem services. The next step in quantifying the ecosystem service of marsh nutrient retention is to apply this method to calculate a long-term mass balance that accounts for seasonal changes in flux and concentrations in tidal marshes.

Acknowledgments

The authors would like to thank the two anonymous reviewers and the editor for their helpful comments on this manuscript. This material is based upon work supported by the National Science Foundation under grant no. DGE-0750733 and the Environmental Protection Agency under grant no. EPA 2871.

References

Anderson, I.C., Tobias, C.R., Neikirk, B.B., Wetzel, R.L., 1997. Development of a process-based nitrogen mass balance model for a Virginia (USA) *Spartina alterniflora* salt marsh: implications for net DIN flux. Mar. Ecol.-Prog. Ser. 159, 13–27.

Aziz, S.A.B.A., Nedwell, D.B., 1986. The nitrogen-cycle of an east-coast, UK salt-marsh. 2. Nitrogen-fixation, nitrification, denitrification, tidal exchange. Estuarine Coastal Shelf Sci. 22, 689–704.

Bayliss-Smith, T., Healey, R., Lailey, R., Spencer, T., Stoddart, D., 1979. Tidal flows in salt marsh creeks. Estuarine Coastal Mar. Sci. 9, 235–255.

Birgand, F., 2000. Quantification and modeling of in-stream processes in agricultural canals of the lower coastal plain. In: Ph.D. Dissertation. North Carolina State University, Raleigh, NC.

Birgand, F., Appelboom, T.W., Chescheir, G.M., Skaggs, R.W., 2011. Estimating nitrogen, phosphorus, and carbon fluxes in forested and mixed-use watersheds of the lower coastal plain of North Carolina: uncertainties associated with infrequent sampling. Trans. ASABE 54 (6), 2099–2110.

Boon, J.D., 1975. Tidal discharge asymmetry in a salt marsh drainage system. Limnol. Oceanogr. 20, 71–80.

Cahoon, D.R., 2006. A review of major storm impacts on coastal wetland elevations. Estuaries Coasts 29, 889–898.

Chalmers, A.G., Wiegert, R.G., Wolf, P.L., 1985. Carbon balance in a salt marsh: Interactions of diffusive export, tidal deposition and rainfall-caused erosion. Estuarine Coastal Shelf Sci. 21, 757–771.

Childers, D.L., Day, J.W., Mckellar, H.N., 2002. Twenty more years of marsh and estuarine flux studies: revisiting nixon (1980). In: Weinstein, M.P., Kreeger, D.A. (Eds.), Concepts and Controversies in Tidal Marsh Ecology. Springer, Netherlands, pp. 391–423.

Christiansen, T., Wiberg, P., Milligan, T., 2000. Flow and sediment transport on a tidal salt marsh surface. Estuarine Coastal Shelf Sci. 50, 315–331.

Chrzanowski, T.H., Stevenson, L.H., Spurrier, J.D., 1982. Transport of particulate organic carbon through the North Inlet ecosystem. Mar. Ecol.-Prog. Ser. 7, 231–245.

Craft, C., Megonigal, P., Broome, S., Stevenson, J., Freese, R., Cornell, J., Zheng, L., Sacco, J., 2003. The pace of ecosystem development of constructed *Spartina alterniflora* marshes. Ecol. Appl. 13, 1417–1432.

Dame, R., Spurrier, J., Williams, T., Kjerve, B., Zingmark, R., 1991. Annual material processing by a salt marsh-estuarine basin in South Carolina, USA. Mar. Ecol.-Prog. Ser. 72, 153–166.

Day, J.W., Psuty, N.P., Perez, B.C., 2002. The role of pulsing events in the functioning of coastal barriers and wetlands: implications for human impact, management and the response to sea level rise. In: Anonymous Concepts and Controversies in Tidal Marsh Ecology. Springer, New York, NY, pp. 633–659.

Etheridge, J.R., 2013. Quantifying the water quality benefits of a constructed brackish marsh and tidal stream system using continuous water quality and flow monitoring. In: Ph.D. Dissertation. North Carolina State University, Raleigh, NC.

Etheridge, J.R., Birgand, F., Osborne, J.A., Osburn, C.L., Burchell, M.R., Irving, J., 2014. Using in situ ultraviolet–visual spectroscopy to measure nitrogen, carbon, phosphorus, and suspended solids concentrations at a high frequency in a brackish tidal marsh. Limnol. Oceanogr. Methods 12, 10–22.

Etheridge, J.R., Birgand, F., Burchell, M.R., Smith, B.T., 2013. Addressing the fouling of in situ ultraviolet–visual spectrometers used to continuously monitor water quality in brackish tidal marsh waters. J. Environ. Qual. 42, 1896–1901.

Fagherazzi, S., Wiberg, P.L., Temmerman, S., Struyf, E., Zhao, Y., Raymond, P.A., 2013. Fluxes of water, sediments, and biogeochemical compounds in salt marshes. Ecol. Processes 2, 1–16.

Gardner, L., Kjerfve, B., 2006. Tidal fluxes of nutrients and suspended sediments at the North Inlet–Winyah Bay National Estuarine Research Reserve. Estuarine Coastal Shelf Sci. 70, 682–692.

Gardner, L.R., Thombs, L., Edwards, D., Nelson, D., 1989. Time series analyses of suspended sediment concentrations at North Inlet, South Carolina. Estuaries 12, 211–221.

Gardner, W.S., McCarthy, M.J., An, S.M., Sobolev, D., Sell, K.S., Brock, D., 2006. Nitrogen fixation and dissimilatory nitrate reduction to ammonium (DNRA) support nitrogen dynamics in Texas Estuaries. Limnol. Oceanogr. 51, 558–568.

Hopkinson, C.S., Giblin, A.E., 2008. Nitrogen dynamics of coastal salt marshes. In: Capone, D.G., Bronk, D.A., Mulholland, M.R., Carpenter, E.J. (Eds.), Nitrogen in the Marine Environment. , second ed. Elsevier, Amsterdam, pp. 991–1036.

ISO 15769(E), 2012. Hydrometry—Guidelines for the Application of Acoustic Velocity Meters using the Doppler and Echo Correlation Methods. ISO 15769(E).

ISO 748, 1997. Measurement of Liquid Flow in Open Channel—Velocity-area Methods. ISO 748.

Jordan, T.E., Whigham, D.F., Hofmockel, K.H., Pittek, M.A., 2003. Nutrient and sediment removal by a restored wetland receiving agricultural runoff. J. Environ. Qual. 32, 1534–1547.

Jordan, T.E., Correll, D.L., 1991. Continuous automated sampling of tidal exchanges of nutrients by brackish marshes. Estuarine Coastal Shelf Sci. 32, 527–545.

Jordan, T.E., Pierce, J.W., Correll, D.L., 1986. Flux of particulate matter in the tidal marshes and subtidal shallows of the Rhode River estuary. Estuaries 9, 310–319.

Kirchner, J.W., Feng, X.H., Neal, C., 2000. Fractal stream chemistry and its implications for contaminant transport in catchments. Nature 403, 524–527.

Koop-Jakobsen, K., Giblin, A.E., 2010. The effect of increased nitrate loading on nitrate reduction via denitrification and DNRA in salt marsh sediments. Limnol. Oceanogr. 55, 789–802.

Levesque, V.A., Oberg, K.A., 2012. Computing discharge using the index velocity method. U.S. Geol. Surv. Tech. Methods 3–A23, 148 (Available online at http://pubs.usgs.gov/tm/3a23/).

Mevik, B., Wehrens, R., Liland, K.H., 2011. pls: Partial least squares and principal component regression. In: R Package Version 2.3-0, http://CRAN.R-project.org/package=pls.

National Atmospheric Deposition Program, 2013. NADP/NTN Monitoring Location NC06 2013. National Atmospheric Deposition Program.

Odum, E.P., 1968. A research challenge: evaluating the productivity of coastal and estuarine water. In: Proceedings of the Second Sea Grant Conference, p. 64.

Pellerin, B.A., Saraceno, J.F., Shanley, J.B., Sebestyen, S.D., Aiken, G.R., Wollheim, W.M., Bergamaschi, B.A., 2012. Taking the pulse of snowmelt: in situ sensors reveal seasonal, event and diurnal patterns of nitrate and dissolved organic matter variability in an upland forest stream. Biogeochemistry 108, 183–198.

Poe, A.C., Piehler, M.F., Thompson, S.P., Paerl, H.W., 2003. Denitrification in a constructed wetland receiving agricultural runoff. Wetlands 23, 817–826.

R Core Team, 2013. R: A Language and Environment for Statistical Computing. R Core Team, http://www.R-project.org.

Raisin, G.W., Mitchell, D.S., Croome, R.L., 1997. The effectiveness of a small constructed wetland in ameliorating diffuse nutrient loadings from an Australian rural catchment. Ecol. Eng. 9, 19–35.

Teal, J.M., 1962. Energy flow in the salt marsh ecosystem of Georgia. Ecology 43, 614–624.

Temmerman, S., Govers, G., Wartel, S., Meire, P., 2003. Spatial and temporal factors controlling short-term sedimentation in a salt and freshwater tidal marsh, Scheldt estuary, Belgium, SW Netherlands. Earth Surf. Processes Landforms 28, 739–755.

Tobias, C.R., Anderson, I.C., Canuel, E.A., Macko, S.A., 2001. Nitrogen cycling through a fringing marsh-aquifer ecotone. Mar. Ecol.-Prog. Ser. 210, 25–39.

Turner, R.E., Baustian, J.J., Swenson, E.M., Spicer, J.S., 2006. Wetland sedimentation from hurricanes Katrina and Rita. Science 314, 449–452.

Tzortziou, M., Neale, P.J., Osburn, C.L., Megonigal, J.P., Maie, N., Jaffé, R., 2008. Tidal marshes as a source of optically and chemically distinctive colored dissolved organic matter in the Chesapeake Bay. Limnol. Oceanogr. 53, 148–159.

Whiting, G.J., McKellar, H.N., Spurrier, J.D., Wolaver, T.G., 1989. Nitrogen exchange between a portion of vegetated salt marsh and the adjoining creek. Limnol. Oceanogr. 34, 463–473.

Wolaver, T.G., Whiting, G.J., Dame, R.F., Williams, T.M., Spurrier, J.D., 1988. Bly Creek ecosystem study—nitrogen exchange within a euhaline salt-marsh basin of North Inlet, South Carolina. Mar. Ecol.-Prog. Ser. 49, 107–116.

Wolaver, T.G., Zieman, J.C., Wetzel, R.L., Webb, K.L., 1983. Tidal exchange of nitrogen and phosphorus between a mesohaline vegetated marsh and the surrounding estuary in the lower Chesapeake Bay. Estuarine Coastal Shelf Sci. 16, 321–332.